表12　HIT-6スコア分類とその人数の推移（人）

HIT-6スコア分類		0週	4週	8週	12週
重度の支障	(60点以上)	179	129	111	111
中等度の支障	(56点～59点)	38	59	47	43
軽度の支障	(50点～55点)	15	30	51	49
日常生活に支障なし，ほとんどなし	(49点以下)	3	14	26	32
合　計 (N)		235	232	235	235

表13　MSQ各下位尺度毎のスコアとHIT-6スコアの相関（ピアソンの相関係数）

	0週時	12週時
RR	−0.68	−0.74
RP	−0.63	−0.65
EF	−0.66	−0.69

RR：Role Function-Restrictive, RP：Role Function-Preventive, EF：Emotional Function

ン®錠の継続的な服用においても承認申請時と同程度以上の結果が得られた。また，片頭痛患者が頭痛治療に最も望むものは頭痛の完全な消失（ペインフリー）であると報告されている[22]ことより，頭痛の消失率は片頭痛患者にとって重要な指標となる。本試験において，中等度/重度からの頭痛消失率は，2時間後，4時間後にはそれぞれ33.9％，57.7％であった。一方，片頭痛が軽度であるうちに服用した際の頭痛消失率は2時間後，4時間後にはそれぞれ62.7％，78.0％と中等度/重度からの服用に比較して高い頭痛消失率を示した。これは，イミグラン®錠を片頭痛が中等度/重度の状態で服用しても本薬剤の効果は発揮されるが，片頭痛が軽度の状態のうちに服用することがより効果的であるためだと考えられた。

試験開始前に片頭痛治療薬として鎮痛薬を使用していた患者を対象に，イミグラン®錠に切り替えた際の患者満足度を表10に示した。「とても満足」，「満足」，「まあまあ満足」の3項目を合計したものを“満足した患者の割合”として検討を行った。問2の効果発現の速さに関して満足した患者の割合は24.5％から59.8％に，問5の片頭痛の痛みに対する効果に関して満足した患者の割合は33.8％から71.4％といずれも2倍以上の増加を示し，頭痛改善率および消失率に表される片頭痛の痛みの軽減を裏付けるものと考えられた。また，問7の社会生活に戻ることのできる速さへの満足度の割合は21.6％から65.6％と3倍以上の増加を示し，片頭痛症状の改善が患者の社会生活に良好な影響を与えていることが推察され，イミグラン®錠がHRQOLと患者の社会生活の双方に著明な改善をもたらしたものと考えられた。

近年，片頭痛の病態に感覚の過敏状態を表すアロディニア（allodynia：pain sensitization）の果たす役割が注目され，トリプタン製剤の効果とアロディニアの関係，痛みの感受性の問題が頭痛の病態の中で大きな役割を果たしている可能性が指摘されている[23]。本試験にて頭痛が発現してからイミグラン®錠を服用するまでの時間を図8に示した。イミグラン®錠を服用するまでの時間が15分以下であった割合は29.2％と3割に満たなかったが，1時間を超えてイミグラン®錠を服用した割合は42.3％と最も多く，自身の頭痛の様子を見ながら服用するという傾向がみられた。アロディニアが発現する前，すなわち片頭痛発現早期に痛みを抑えることができれば痛みの連鎖反応を制御することができ，患者の望む頭

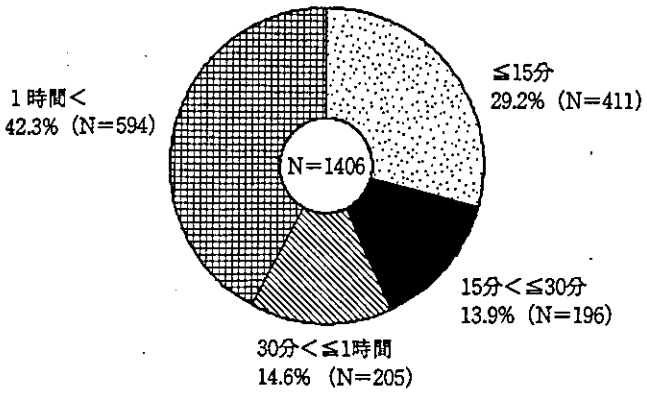

図8　頭痛発現から服薬までの時間

痛消失効果を得ることができると報告されている[24)25)]。本試験においても，前述したように，軽度で服薬した際の頭痛消失率は，中等度/重度に悪化してから服薬した際に比べて高い値を示したことは，この結果を裏付けるものと考えられる。臨床的に治療効果を最大限に発揮させるためにも，早期服薬を含めた適切な患者指導が重要となると考えられる。

表11に示したとおり，副作用発現症例率は32.5％であり，その主な事象は，悪心（10.1％），倦怠感（6.3％），圧迫感（4.2％），動悸（3.4％）であった。本試験でみられた副作用はいずれも承認申請時の副作用と同様のものであった。悪心は本剤の服用後に発現していることから本剤の副作用として挙げられたが，表5に示したように片頭痛の随伴症状として悪心が多いことから，これらが随伴症状であった可能性もあると考えられた。また圧迫感はその多くが肩や頚部の圧迫感であり，これらに関しても片頭痛の随伴症状や緊張型頭痛に伴うものであった可能性も考えられた。トリプタン製剤に特有の副作用と考えられている胸部不快感および胸痛についての副作用発現症例率は本試験ではそれぞれ2.1％，2.5％であったが，承認申請時ではそれぞれ0.7％，1.3％であった。本試験では承認申請時のように単回のみの服用ではなく，12週間の試験期間中平均8.3錠を服用しているが，複数回の服用で1度でも副作用の発現した患者は副作用発現症例数に組み込まれていることが副作用発現症例率に影響していると考えられた。他のトリプタン製剤の添付文書[26)~28)]においても，胸部症状については1～4％とイミグラン®錠と同程度の発現頻度が報告されており，本試験での発現率は臨床的に問題となるものではないと考えられた。

以上より，イミグラン®錠の継続的な投与により頭痛の改善・消失効果が得られるのみではなく，片頭痛によって低下したHRQOLの改善および高い患者満足度が得られることが確認され，イミグラン®錠はHRQOLの向上に対して有用性を発揮し，継続使用に対する安全性についても良好な薬剤であると考えられた。また，HIT-6は片頭痛患者が定期的に自身の片頭痛による日常生活への支障度を測定するためのツールとして優れ，医師が片頭痛患者の視点に立った治療を行うための一助となると考えられた。

ま と め

本試験は片頭痛患者のHRQOL改善を目的とした多施設共同臨床試験であり，以下のことが確認された。

・イミグラン®錠投与によりMSQスコアは有意に改善（$p<0.0001$）し，日常役割機能の制限，日常役割機能の妨害，感情的機能の全ての尺度においてHRQOLが向上する。

・イミグラン®錠投与によりHIT-6スコアは有意に改善（$p<0.0001$）し，片頭痛患者の仕事や家庭，学校や社会生活に対する支障度が改善される。

・鎮痛薬中心の片頭痛治療からイミグラン®錠による治療に切り替えた場合，HRQOLは十分に改善される。

・鎮痛薬と比較してイミグラン®錠は高い患者満足度が確認され，特に片頭痛の痛みに対する効果，社会生活に戻ることのできる速さはそれぞれ71.4％，65.6％の患者において満足を示した。

・イミグラン®錠の服用による頭痛改善率は，服用2時間後，4時間後にそれぞれ75.8％，80.0％，頭痛消失率（中等度/重度）は2時間後，4時間後にそれぞれ33.9％，57.7％である。

・HIT-6スコアはMSQスコアと十分な相関（ピアソンの相関係数：－0.63～－0.74）を示し，また使用に際して簡便であることから，HIT-6は定期的に片頭痛患者の日常生活の支障度を測定するツールとして優れていると考えられた。

・イミグラン®錠は継続的に服用する際においても安全性は良好である。

謝　辞

本試験に御参画頂いた試験責任医師，分担医師，試験コーディネーター他医療関係者の方々，並びに試験依頼者であるグラクソ・スミスクライン株式会社の関係者の方々に厚く御礼申し述べたい。

文　献

1) Sakai, F., Igarashi, H.：Prevalence of migraine in Japan：a nationwide survey. Cephalalgia 17：15-22, 1997.
2) Igarashi, H., Sakai, F.：Current status of diagnosis and treatment of migraine headache in Japanese women. Headache Care, 1(3)：207-213, 2004.
3) Gross, M.L.P., Dowson, A.J., Deavy, L., et al.：Impact of oral sumatriptan 50mg on work productivity and quality of life in migraineurs. Brit J Med Econ, 10：231-246, 1996.
4) Jhingran, P., Cady, R. K., Rubino, J., et al.：Improvements in health-related quality of life with sumatriptan treatment for migraine：J Fam Pract 42：36-42, 1996.
5) Munshet, G. R., Miller. D., Clements. B., et al.：Impact of sumatriptan on workplace productivity, nonwork activities, and health-related quality of life among hospital employees with migraine. Headache, 36：137-143, 1996.
6) Jhingran. P., Osterhaus. J. T., Miller. D. W., et al.：Development and validation of the migraine-specific quality of life questionnaire. Headache, 38：295-302, 1998.
7) 坂井文彦，福内靖男，岩田誠，他：日本語版片頭痛用quality of life調査書の信頼性と妥当性の検討，神経治療，21：449-458, 2004.
8) Bayliss; M.S., Batenhorst, A.S.：The HIT-6 a user's guide：Quality Metric Incorporated, June 2002.
9) International Headache Society：Cephalalgia 8 (Suppl 7), 9, 12-17, 19-17, 75-92, 1988.
10) 坂井文彦，福内靖男，岩田誠，他：日本語版Headache Impact Test（HIT-6）の信頼性の検討，臨床医薬，20(10)：1045-1054, 2004.
11) 濱田潤一，清水俊彦，福内靖男，他：日本語版片頭痛用quality of life調査書の言語的妥当性の検討，神経治療，21：443-447, 2004.
12) 片頭痛の具体的な医療手順に関する調査：研究平成15年度総括・分担研究報告書, 2004.
13) Osterhaus, J. T., Townsend, R. J., Gandek, B., et al.：Measuring the functional status and well-being of patients with migraine headache. Headache, 34：337-343, 1994.
14) 竹島多賀夫，森望美，粟木悦子，他：慢性頭痛患者のQuality of life（QOL）第2報．日本頭痛学会誌26(1)：12-14, 1999.
15) Terwindt, G. M., Ferrari, M. D., Tijhuis, M., et al.：The impact of migraine on quality of life in the general population-The GEM study. Neurology, 55：624-629, 2000.
16) Lofland, J. H., Johnson, N. E., Batenhorst, A. S., et al.：Changes in resource use and outcomes for patients with migraine treated with sumatriptan：Arch Intern Med, 159：857-863, 1999.
17) Chassany, O., Sagnier, P., Marquis, P., et al.：Patient-reported outcomes：The example of health-related quality of life：Drug Information Journal, 36：209-238. 2002.
18) Dowson, A., Dahlof, C., Tepper, S., et al.：Prevalence and diagnosis of migraine in a primary care setting. Poster presented at, The 14th Migraine Trust International Symposium. 2002.
19) 竹島多賀夫，五十嵐久佳：片頭痛症状の訴え方．診断と治療，92(6)：1075-1080. 2004.
20) Holmes, W. F., MacGregor, E. A., Sawyer, JPC., et al.：Information about migraine disability influences physicians'perceptions of illness severity and treatment needs：Headache, 41：343-350, 2001.
21) 坂井文彦，岩田誠，松本清，他：コハク酸スマトリプタン錠（GW102）の後期第II相臨床試験，臨床医薬，17(8)：1163-1187, 2001.
22) Leinisch-Dahlke, E., Akova-Öztürk, E., Bertheau, U. et al.：Patient preference in clinical trials for headache medication：Cephalalgia 24：347-355, 2004.
23) 坂井文彦：頭痛の診断と治療最新Version, Medical ASAHI, Sep.：65-69, 2004.
24) Burstein, R., Yarnitsky, D., Goor-Aryeh, I.,et al.：An association between migraine and cutaneous allodynia, Ann Neurol, 47：614-624, 2000.

25) Burstein, R., Cutrer, M.F., Yarnitsky, D., et al. : The development of cutaneous allodynia during a migraine attack, Brain, 123 : 1703-1709, 2000.
26) Zolmitriptan (Zomig) US Pis.
27) Rizatriptan (Maxalt) US Pis.
28) Eletriptan (RELPAX) US Pis.

ELSEVIER

Clinical Neurophysiology 115 (2004) 1857–1862

www.elsevier.com/locate/clinph

Somatosensory evoked high-frequency oscillations in migraine patients

Kenji Sakuma[a,b,*], Takao Takeshima[b], Kumiko Ishizaki[b], Kenji Nakashima[b]

[a]*Section of Environment and Health Science, Department of Biological Regulation, School of Health Sciences, Faculty of Medicine, Tottori University, 86 Nishimachi, Yonago, Japan*

[b]*Division of Neurology, Faculty of Medicine, Institute of Neurological Sciences, Tottori University, 36-1 Nishimachi, Yonago 683-8504, Japan*

Accepted 9 March 2004

Abstract

Objective: To explore additional evidence concerning generators of somatosensory evoked high-frequency oscillations (HFOs).

Methods: We recorded HFOs in migraine patients. Subjects were 19 healthy normal subjects and 19 migraineurs. Electrical stimuli were delivered alternately to the right and left median nerves at their wrists. EEGs were recorded from C3′-Fz, C4′-Fz, Erb1–Erb2, Erb2–Erb1 and Cv6-Fz using a 0.3 Hz low-frequency filter and a 3000 Hz high-frequency filter. Responses to 5000 stimuli were averaged. For separation of HFOs from underlying N20, the digitized wide-band signals were digitally bandpass filtered (400–800 Hz) and averaged.

Results: There were no significant differences in peak latencies and amplitudes for N9, N13, N20 and P25 components between normal controls and migraineurs. Root-mean-square amplitudes for HFOs in migraineurs were significantly diminished compared with normal controls.

Conclusions: A diminished inhibitory mechanism in the somatosensory system may exist in migraineurs. It remains to determine what cell populations contribute to generating HFOs.

Significance: This indicates that there is a dysfunction in cortical information processing in the somatosensory cortex of migraineurs.

Keywords: Somatosensory evoked potentials; High-frequency oscillations; Migraine; Inhibitory interneurons; Sodium valproate; Gamma-aminobutyric acid

1. Introduction

Migraine is a common form of head pain, with a prevalence of 15% in Western Europe. Neurophysiological investigations are a useful non-invasive method for attempting to understand the pathophysiology of migraine. Studies using sensory evoked potentials and transcranial magnetic stimulation have disclosed abnormalities of cortical excitability in migraine patients (Ambrosini et al., 2003). These studies have focused mainly on the visual system. Somatic evoked potentials do not show habituation in migraine patients (Ozkul and Uckardes, 2002). This indicates that there is a dysfunction in cortical information processing not only in the visual cortex, but also in the somatosensory cortex.

Low-amplitude, high-frequency primary cortical oscillations in the frequency range of 500–800 Hz superimposed on the ascending slope of the N20 primary response following stimulation of the median nerve have been reported (Curio et al., 1994; Hashimoto et al., 1996b; Yamada et al., 1988). Although several studies using electroencephalography (EEG) or magnetoencephalography (MEG) have provided a wide range of information about the generator of these high frequency wavelets: from thalamus (Eisen et al., 1984; Klostermann et al., 2002), thalamocortical presynaptic action potentials (Gobbele et al., 1998) to somatosensory cortex (Curio et al., 1997; Hashimoto et al., 1999; Sakuma et al., 1999; Shimazu et al., 2000), the precise anatomical location of the generator remains unclear. The second point of debate is the physiological mechanism of the high-frequency oscillations (HFOs) generation. Although it is generally supposed that the N20 component is generated by excitatory postsynaptic potentials (EPSPs) of pyramidal neurons in area 3b, specialized neuronal classes in the somatosensory cortex

* Corresponding author. Address: Division of Neurology, Faculty of Medicine, Institute of Neurological Sciences, Tottori University, 36-1 Nishimachi, Yonago 683-8504, Japan. Tel.: +81-859-34-8032; fax: +81-859-34-8083.

E-mail address: neurol@smile.ocn.ne.jp (K. Sakuma).

1388-2457/$30.00
doi:10.1016/j.clinph.2004.03.011

are presumed to be related to HFO generation. The cell populations convincingly proposed to be involved in HFO generation are 'chattering cells' in layer III, fast-spiking GABAergic inhibitory interneurons, regular-spiking cells and intrinsically bursting cells (Curio, 2000). The anatomical and physiological origins of HFOs are still a matter of considerable debate.

In this study, we recorded somatosensory evoked HFOs in patients with migraine to explore additional evidence concerning HFO generators.

2. Subjects and methods

Nineteen healthy normal subjects (12 females and 7 males; mean age 34.4 years, range 20–75 years) and 19 age-matched patients with migraine recruited from a specialized headache clinic (14 females and 5 males; mean age 38.5 years, range 15–67 years) were studied. Migraine was diagnosed according to the International Headache Society criteria. The migraine group comprised patients with migraine with aura (code 1.2; MA; $n = 6$) and migraine without aura (code 1.1; MO; $n = 13$) (Table 1). Patients received no prophylactic therapy or sodium valproate. Recordings were taken during attack-free intervals. At least a 3-day attack-free phase before and after the study was verified from each participant's record. Informed consent was obtained from each participant prior to the study.

Electrical stimuli with a 0.2 ms duration were delivered alternately to the right and left median nerve at the subjects' wrists (cathode proximal). The stimulus intensity was set at 3 times the sensory threshold. The stimuli were delivered at irregular intervals with intervals between 211 and 262 ms. Recording electrodes were placed on C3′, C4′ (2 cm posterior to C3, C4), Fz of the International 10–20 System, Erb1, Erb2 and the sixth cervical spinous process (Cv6). Electrode impedance was maintained below 5 kΩ. EEG was recorded from C3′-Fz, C4′-Fz, Erb1–Erb2, Erb2–Erb1 and Cv6-Fz using a 0.3 Hz low-frequency filter and a 3000 Hz high-frequency filter, then digitized with an analogue to digital converter (micro1401, CED, Cambridge, UK) at a sampling rate of 20 kHz and stored on disk for further analysis. We used C3′-Fz montage for recording HFOs because it is known to be the best method from our experience and previous studies (Mochizuki et al., 1999). An epoch of 50 ms duration was obtained sequentially. Responses to 5000 stimuli were averaged offline using Spike2 software (CED, Cambridge, UK). For separation of HFOs from underlying N20, the digitized wide-band signal was digitally bandpass filtered (400–800 Hz), and averaged.

Table 1
Characteristics of migraineurs

Feature	Migraine ($n = 19$)
Sex	
Female	14
Male	5
Age, mean (SD) (years)	38.5 (17.6)
Type of headache	
Migraine with aura	6
Migraine without aura	13
Headache frequency (attacks/month)	
< 3	8
3	2
4	2
> 4	7
Duration of attacks (h)	
< 12	3
12–24	4
25–48	10
49–72	2

In wide-band recordings, N20 onset latency, amplitudes and peak latencies for N9, N13, N20 and P25 components were measured and analyzed.

The size of HFOs was calculated from their root-mean-square (RMS) amplitude from the onset to the offset of the HFOs. Onset/offset criteria for HFOs was where they exceeded the averaged background noise level for the subject's control session by 3SD. The number of negative peaks was also counted. All these parameters were separated into two parts: (1) the first half of HFOs (onset to N20 peak) and (2) the latter half (N20 peak to endpoint).

A one-way analysis of variance (ANOVA) was employed to analyze somatosensory evoked potentials (SEPs) and HFO data from the patients and normal control subjects. Post hoc comparisons were made using the Bonferroni method. A value of $P < 0.05$ was considered to be statistically significant.

3. Results

3.1. Conventional somatosensory evoked potentials

In all subjects N9, N13, N20 and P25 were clearly identified in wide-band recordings. There were no significant differences in peak latencies and amplitudes between normal controls and migraineurs (Table 2).

3.2. Number of HFO peaks

Fig. 1 shows a typical SEP waveform obtained by wide-band recording. In the ascending and descending slope of the cortical N20 response, small notches, which were thought to be HFOs, were detected (open triangles). After applying a 400–800 Hz digital filter, HFOs superimposed on N20 were clearly identified (Fig. 1, arrows). Though the number of HFO peaks had a tendency to be smaller in migraineurs, the difference did not reach statistical significance (Table 3, Fig. 2).

Table 2
Wide-band SEPs

	Normal ($n = 19$)	MA ($n = 6$)	MO ($n = 13$)	MA + MO ($n = 19$)
SEPs by right median nerve				
N20 onset latency (ms)	14.97 ± 0.89	15.41 ± 1.40	14.50 ± 1.12	14.79 ± 1.25
N20 peak latency (ms)	18.86 ± 0.95	19.04 ± 1.43	18.51 ± 0.95	18.68 ± 1.11
P25 peak latency (ms)	23.99 ± 2.58	24.54 ± 3.22	24.59 ± 2.50	24.57 ± 2.65
N20 duration (N20 onset–N20 peak) (ms)	3.89 ± 0.81	3.63 ± 0.48	4.00 ± 0.69	3.89 ± 0.64
P25 duration (N20 peak–P25 peak) (ms)	5.13 ± 2.35	5.50 ± 2.02	6.08 ± 2.03	5.90 ± 1.99
N20 amplitude (μV)	2.07 ± 1.79	1.75 ± 1.34	2.59 ± 2.26	2.32 ± 2.02
P25 amplitude (μV)	5.19 ± 6.25	1.96 ± 0.87	2.02 ± 1.18	2.00 ± 1.07
N9 latency (ms)	9.41 ± 0.68	9.39 ± 0.29	8.86 ± 0.60	9.04 ± 0.57
N9 amplitude (μV)	3.49 ± 2.07	4.47 ± 2.32	5.64 ± 2.21	5.25 ± 2.24
SEPs by left median nerve				
N20 onset latency (ms)	15.23 ± 0.91	14.12 ± 0.76	14.66 ± 1.14	14.49 ± 1.04
N20 peak latency (ms)	18.79 ± 1.18	18.11 ± 0.90	18.37 ± 1.02	18.29 ± 0.97
P25 peak latency (ms)	24.3 ± 2.87	23.77 ± 1.82	24.70 ± 1.79	24.40 ± 1.80
N20 duration (N20 onset–N20 peak) (ms)	3.56 ± 0.98	3.98 ± 0.54	3.71 ± 0.66	3.80 ± 0.62
P25 duration (N20 peak–P25 peak) (ms)	5.51 ± 2.64	5.66 ± 1.33	6.33 ± 1.64	6.12 ± 1.55
N20 amplitude (μV)	2.59 ± 1.44	2.23 ± 0.68	2.25 ± 1.83	2.24 ± 1.54
P25 amplitude (μV)	4.17 ± 4.79	2.70 ± 1.55	1.80 ± 1.60	2.08 ± 1.60
N13 latency (ms)	12.97 ± 1.02	12.71 ± 0.36	12.05 ± 1.19	12.26 ± 1.04
N13 amplitude (μV)	1.76 ± 1.16	2.94 ± 0.76	2.58 ± 0.76	2.70 ± 0.76
N9 latency (ms)	9.36 ± 0.68	9.07 ± 0.42	8.80 ± 0.68	8.88 ± 0.61
N9 amplitude (μV)	4.92 ± 2.37	3.71 ± 0.79	4.74 ± 2.52	4.42 ± 2.15

Means ± SD.

3.3. RMS amplitude of HFOs

The mean value of RMS amplitude of HFOs was significantly lower in migraineurs than controls (0.098 vs. 0.063 from C3′ electrode and 0.097 vs. 0.059 from C4′ electrode) ($P < 0.05$). The late part, as well as the early part, of HFOs showed a significant reduction in RMS amplitude in migraine patients (Table 3, Fig. 2).

3.4. Aura

Migraineurs were divided into two groups: those with (MA) and those without (MO) aura. There were 6 MA patients and 13 MO patients (Table 1). None of the parameters for SEP components or HFO components showed any significant difference between the two groups (Tables 2 and 3). Though the RMS amplitudes for HFOs

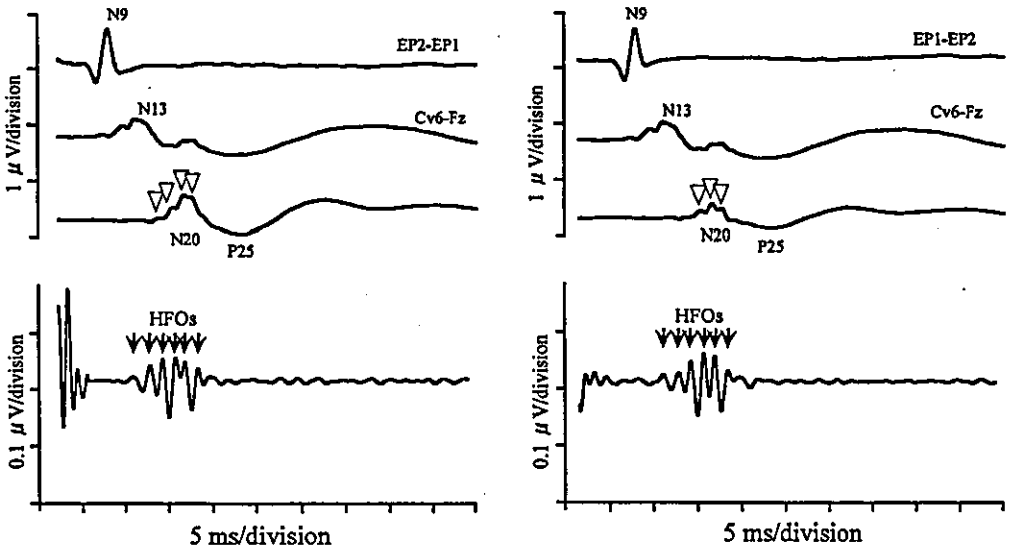

Fig. 1. Typical waveforms for SEPs and HFOs stimulated by right median nerves (left) and left median nerves (right). On the ascending slope of the cortical N20 component, small notches that correspond to HFO components are detected.

Table 3
HFO parameters in normals and patients

	Normal ($n = 19$)	MA ($n = 6$)	MO ($n = 13$)	MA + MO ($n = 19$)
HFOs by right median nerve				
HF Nr of peaks	5.56 ± 1.76	4.83 ± 0.98	5.08 ± 1.32	5.00 ± 1.20
HF Nr of peaks (onset–N20 peak)	3.33 ± 1.28	2.50 ± 0.55	3.08 ± 1.26	2.89 ± 1.10
HF Nr of peaks (N20 peak–endpoint)	2.22 ± 1.26	2.33 ± 0.52	2.00 ± 1.35	2.11 ± 1.15
RMS of HF	0.098 ± 0.055	0.065 ± 0.008	0.062 ± 0.027	0.063 ± 0.023*
RMS of HF (onset–N20 peak)	0.106 ± 0.05	0.073 ± 0.021	0.054 ± 0.031*	0.060 ± 0.029*
RMS of HF (N20 peak–endpoint)	0.096 ± 0.05	0.064 ± 0.018	0.063 ± 0.027	0.063 ± 0.024*
HFOs by left median nerve				
HF Nr of peaks	5.06 ± 1.89	4.67 ± 0.82	4.54 ± 1.56	4.58 ± 1.35
HF Nr of peaks (onset–N20 peak)	2.41 ± 1.50	3.00 ± 1.26	3.00 ± 1.22	3.00 ± 1.20
HF Nr of peaks (N20 peak–endpoint)	2.65 ± 1.41	1.67 ± 0.82	1.54 ± 1.05	1.58 ± 0.96
RMS of HF	0.097 ± 0.057	0.074 ± 0.013	0.053 ± 0.027*	0.059 ± 0.025*
RMS of HF (onset–N20 peak)	0.100 ± 0.076	0.062 ± 0.019	0.059 ± 0.029*	0.060 ± 0.026*
RMS of HF (N20 peak–endpoint)	0.106 ± 0.049	0.073 ± 0.030	0.055 ± 0.037*	0.061 ± 0.035*

Means ± SD. *$P < 0.05$ vs. control.

tended to be small in MA compared with normal controls, the difference did not reach statistical difference (Table 3).

4. Discussion

In this study, EEG HFOs in migraine patients were diminished in amplitude, but uncorrelated with aura.

Several lines of research concerning the high frequency oscillation superimposed mainly on the ascending slope of the N20 primary cortical responses of median SEPs have been followed. Reported generators for the HFOs are as follows: thalamus (Eisen et al., 1984), thalamocortical radiation (Gobbele et al., 1999; Yamada et al., 1988) and cortex (Curio et al., 1997; Hashimoto et al., 1996a, 1999; Sakuma and Hashimoto, 1999; Sakuma et al., 1999). However, the origin of HFOs remains controversial. Possible cell populations generating high frequency bursts have been proposed, such as pyramidal chattering cells, cortical fast-spiking inhibitory interneurons and some thalamocortical relay cells. HFOs vary morphologically during the sleep–wake cycle (Emerson et al., 1988; Hashimoto et al., 1996b; Yamada et al., 1988). They show a marked attenuation in amplitude and also a reduction in the number of peaks, while the N20m amplitude exhibited a moderate increment during sleep (Hashimoto et al., 1996b). Based on the reciprocal relationship between HFOs and N20m representing ensemble EPSPs of the pyramidal neurons in the 3b area, it has been postulated that the HFOs represent a localized activity of GABAergic inhibitory interneurons in layer 4 of area 3b (Hashimoto et al., 1996b). In animal studies, inhibitory interneurons of the primary sensory cortex receive a potent monosynaptic thalamic input (Swadlow, 1995). Using an intracellular recording method, inhibitory interneurons have been identified by a high-frequency (>600 Hz) burst of 3 or more spikes elicited by thalamic stimulation (Swadlow et al., 1998). These characteristics were seen in GABAergic fast-spiking non-pyramidal cells which show repetitive firing without adaptation. These animal data are consistent with human HFO data.

The attenuation of the N20 primary response of SEPs by simultaneous tactile stimulation of the hand (Kakigi et al., 1995) or by exploratory finger movements of the hand

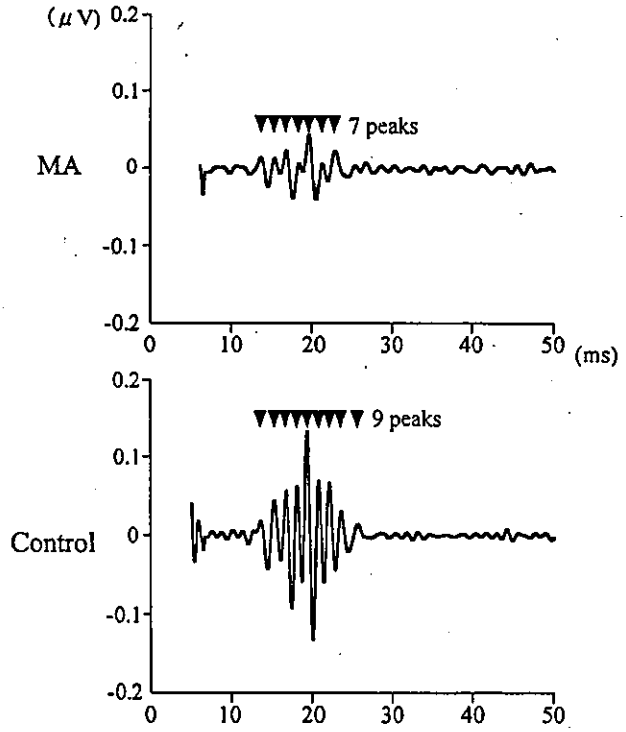

Fig. 2. HFOs obtained from a migraineur without aura (top) and a normal control (bottom). The number of HFO peaks is relatively smaller in the MO patient than in the normal control (7 vs. 9 peaks). The amplitude of HFOs in MO is attenuated compared with that in normal controls.

(Schnitzler et al., 1995) is known as 'gating'. By interfering with palm-brushing stimulation, the number of HFO peaks increases moderately, whereas N20m amplitude decreases dramatically (Hashimoto et al., 1999). Similarly, the HFO/N20m amplitude index was greater in a finger movement task (Tanosaki et al., 2002). Another study showed that HFOs were modulated neither in amplitude nor in latency by isometric motor interference, though the N20 and P25 component of SEPs was attenuated (Klostermann et al., 2001). The discrepancies between N20 and HFO amplitudes by interference are additional evidence supporting the inhibitory interneuron theory as an HFO generator (Hashimoto et al., 1999; Tanosaki et al., 2002). On the other hand, other studies have provided evidence that other cell populations contribute to generating HFOs. 'Chattering' pyramidal cells in layer III can discharge with intraburst frequencies as high as 800 Hz (Gray and McCormick, 1996). The probability of detecting chattering cells in cortical slices was enhanced by cholinergic agonists. Recently, it was shown that HFOs were significantly enhanced after administration of rivastigmine, an acetylcholinesterase inhibitor (Restuccia et al., 2003). It is known that GABAergic cells are also influenced by acetylcholine. Cholinergic or muscarinic agonists induce GABAergic postsynaptic currents. However, there are several GABAergic cell subtypes having different physiological functions. Fast-spiking GABAergic cells containing the calcium-binding protein parvalbumin, proposed as candidates for HFO generator cells, were not influenced by a cholinergic agonist (Kawaguchi, 1997). Consequently, Restuccia concluded that chattering pyramidal cells rather than GABAergic fast-spiking cells play a significant role in the generation of high-frequency spike bursts (Restuccia et al., 2003).

Studies with transcranial magnetic stimulation have provided important, but rather controversial, information about changes in excitability of cerebral cortex in migraine patients (Ambrosini et al., 2003). Several studies showed that the magnetophosphene threshold was lower in migraineurs than in controls (Aurora et al., 1998). This phenomenon can be interpreted as increased excitability of the visual cortex. One explanation for cortical dysfunction on the basis of reduced magnetophosphene threshold in migraineurs is that a loss of GABAergic interneurons may result from hypoxic stress after cortical spreading depression (Chronicle and Mulleners, 1994; Romijn et al., 1988; Sloper et al., 1980). This hypothesis is reinforced by a report of normalized abnormal phosphene threshold after administration of sodium valproate (Mulleners et al., 2002).

Serotonergic dysfunction is one of the important theories in migraine pathophysiology. Long standing studies of evidence-linking serotonin to migraine have led to the development of triptans, which are selective 5-$HT_{1B/1D}$ agonists. The triptans have profoundly improved the quality of life of patients with migraine. It is well known that there is an interaction between cholinergic and serotonergic systems in the brain (Bianchi et al., 1990). Based on these findings, Nicolodi et al. (2002) used donepezil, a cholinesterase inhibitor, expecting an antinociceptive activity in migraine and found it to be effective. This basic and clinical evidence indirectly indicates that migraineurs may have a cholinergic dysfunction in connection with a serotonergic one.

Several studies have shown that HFOs are not homogeneous. Magnetoencephalographic studies have indicated that the current source of HFOs is located in area 3b of S-I and had tight somatotopical arrangement (Curio et al., 1997; Hari and Forss, 1999; Sakuma and Hashimoto, 1999; Sakuma et al., 1999). Recording by magnetoencephalography is limited, in that only the tangential dipole can be recorded. However, using multiple channel EEG recording, current sources, which are thought to be located on area I, having radial direction of HFOs about 22 ms in latency were successfully detected (Ozaki et al., 1998). The early part of the HFOs with the latency range of 13–18 ms distribute over the whole scalp with the same polarity, which probably reflects a subcortical origin (Restuccia et al., 2003). In this study, a change in HFO parameters was observed, not only in the late part of the HFO component, but also in the early part of the HFO component. It is possible to establish two hypotheses. First, that the same pathophysiological mechanism plays a role in the change of both subcortical and cortical HFOs in migraine. Second, that dysfunction of subcortical HFO generators causes a bottom-up regulation of cortically generated HFOs. An alternative interpretation of these results is that the method we used to separate the early and the late parts of the HFOs differed from other studies. By using multiple electrodes, the early and late part of HFOs could be distinguished with and without phase reversal (Ozaki et al., 1998; Restuccia et al., 2003). Since a single recording electrode for cortical response was used in this study, we separated the two parts with the latency of the N20 peak. This method may result in a misjudgment of the boundary between the early and late part of HFOs.

It remains to be determined if fast-spiking cells or chattering cells contribute to the generation of HFOs, and there is the possibility that both cell populations contribute equally. There is considerable support for the theory that both GABAergic and cholinergic dysfunction exist in the cortex of migraineurs. Prophylactic effects of sodium valproate are reported not only in MA patients, but also in MO patients (Jensen et al., 1994; Kaniecki, 1997). It is postulated that a dysfunction in the GABA system exists in both MO and MA patients and furthermore, that this dysfunction is long-lasting and remains in the interictal phase. Both GABAergic anticonvulsants (Leniger et al., 2000; Mathew et al., 2000) and a cholinesterase inhibitor (Nicolodi et al., 2002) have antimigraine efficacy. Interventions with these drugs may provide further understanding of the nature of HFO generation.

References

Ambrosini A, de Noordhout AM, Sandor PS, Schoenen J. Electrophysiological studies in migraine: a comprehensive review of their interest and limitations. Cephalalgia 2003;23(1):13–31.

Aurora SK, Ahmad BK, Welch KM, Bhardhwaj P, Ramadan NM. Transcranial magnetic stimulation confirms hyperexcitability of occipital cortex in migraine. Neurology 1998;50:1111–4.

Bianchi C, Siniscalchi A, Beani L. 5-HT1A agonists increase and 5-HT3 agonists decrease acetylcholine efflux from the cerebral cortex of freely-moving guinea-pigs. Br J Pharmacol 1990;101:448–52.

Chronicle E, Mulleners W. Might migraine damage the brain? Cephalalgia 1994;14:415–8.

Curio G. Linking 600-Hz "spikelike" EEG/MEG wavelets (sigma-bursts) to cellular substrates: concepts and caveats. J Clin Neurophysiol 2000;17: 377–96.

Curio G, Mackert BM, Burghoff M, Koetitz R, Abraham-Fuchs K, Harer W. Localization of evoked neuromagnetic 600 Hz activity in the cerebral somatosensory system. Electroencephalogr Clin Neurophysiol 1994;91:483–7.

Curio G, Mackert BM, Burghoff M, Neumann J, Nolte G, Scherg M, Marx P. Somatotopic source arrangement of 600 Hz oscillatory magnetic fields at the human primary somatosensory hand cortex. Neurosci Lett 1997;234:131–4.

Eisen A, Roberts K, Low M, Hoirch M, Lawrence P. Questions regarding the sequential neural generator theory of the somatosensory evoked potential raised by digital filtering. Electroencephalogr Clin Neurophysiol 1984;59:388–95.

Emerson RG, Sgro JA, Pedley TA, Hauser WA. State-dependent changes in the N20 component of the median nerve somatosensory evoked potential. Neurology 1988;38:64–8.

Gobbele R, Buchner H, Curio G. High-frequency (600 Hz) SEP activities originating in the subcortical and cortical human somatosensory system. Electroencephalogr Clin Neurophysiol 1998;108:182–9.

Gobbele R, Buchner H, Scherg M, Curio G. Stability of high-frequency (600 Hz) components in human somatosensory evoked potentials under variation of stimulus rate—evidence for a thalamic origin. Clin Neurophysiol 1999;110:1659–63.

Gray CM, McCormick DA. Chattering cells: superficial pyramidal neurons contributing to the generation of synchronous oscillations in the visual cortex. Science 1996;274:109–13.

Hari R, Forss N. Magnetoencephalography in the study of human somatosensory cortical processing. Philos Trans R Soc Lond B Biol Sci 1999;354:1145–54.

Hashimoto I, Mashiko T, Imada T. High-frequency magnetic signals in the human somatosensory cortex. Electroencephalogr Clin Neurophysiol Suppl 1996a;47:67–80.

Hashimoto I, Mashiko T, Imada T. Somatic evoked high-frequency magnetic oscillations reflect activity of inhibitory interneurons in the human somatosensory cortex. Electroencephalogr Clin Neurophysiol 1996b;100:189–203.

Hashimoto I, Kimura T, Fukushima T, Iguchi Y, Saito Y, Terasaki O, Sakuma K. Reciprocal modulation of somatosensory evoked N20m primary response and high-frequency oscillations by interference stimulation. Clin Neurophysiol 1999;110:1445–51.

Jensen R, Brinck T, Olesen J. Sodium valproate has a prophylactic effect in migraine without aura: a triple-blind, placebo-controlled crossover study. Neurology 1994;44:647–51.

Kakigi R, Koyama S, Hoshiyama M, Watanabe S, Shimojo M, Kitamura Y. Gating of somatosensory evoked responses during active finger movements magnetoencephalographic studies. J Neurol Sci 1995;128: 195–204.

Kaniecki RG. A comparison of divalproex with propranolol and placebo for the prophylaxis of migraine without aura. Arch Neurol 1997;54:1141–5.

Kawaguchi Y. Selective cholinergic modulation of cortical GABAergic cell subtypes. J Neurophysiol 1997;78:1743–7.

Klostermann F, Gobbele R, Buchner H, Siedenberg R, Curio G. Differential gating of slow postsynaptic and high-frequency spike-like components in human somatosensory evoked potentials under isometric motor interference. Brain Res 2001;922:95–103.

Klostermann F, Gobbele R, Buchner H, Curio G. Intrathalamic non-propagating generators of high-frequency (1000 Hz) somatosensory evoked potential (SEP) bursts recorded subcortically in man. Clin Neurophysiol 2002;113:1001–5.

Leniger T, Wiemann M, Bingmann D, Hufnagel A, Bonnet U. Different effects of GABAergic anticonvulsants on 4-aminopyridine-induced spontaneous GABAergic hyperpolarizations of hippocampal pyramidal cells—implication for their potency in migraine therapy. Cephalalgia 2000;20:533–7.

Mathew NT, Kailasam J, Meadors L, Chernyshev O, Gentry P. Intravenous valproate sodium (Depacon) aborts migraine rapidly: a preliminary report. Headache 2000;40:720–3.

Mochizuki H, Ugawa Y, Machii K, Terao Y, Hanajima R, Furubayashi T, Uesugi H, Kanazawa I. Somatosensory evoked high-frequency oscillation in Parkinson's disease and myoclonus epilepsy. Clin Neurophysiol 1999;110:185–91.

Mulleners WM, Chronicle EP, Vredeveld JW, Koehler PJ. Visual cortex excitability in migraine before and after valproate prophylaxis: a pilot study using TMS. Eur J Neurol 2002;9:35–40.

Nicolodi M, Galeotti N, Ghelardini C, Bartolini A, Sicuteri F. Central cholinergic challenging of migraine by testing second-generation anticholinesterase drugs. Headache 2002;42:596–602.

Ozaki I, Suzuki C, Yaegashi Y, Baba M, Matsunaga M, Hashimoto I. High frequency oscillations in early cortical somatosensory evoked potentials. Electroencephalogr Clin Neurophysiol 1998;108:536–42.

Ozkul Y, Uckardes A. Median nerve somatosensory evoked potentials in migraine. Eur J Neurol 2002;9:227–32.

Restuccia D, Della Marca G, Valeriani M, Rubino M, Paciello N, Vollono C, Capuano A, Tonali P. Influence of cholinergic circuitries in generation of high-frequency somatosensory evoked potentials. Clin Neurophysiol 2003;114:1538–48.

Romijn HJ, Ruijter JM, Wolters PS. Hypoxia preferentially destroys GABAergic neurons in developing rat neocortex explants in culture. Exp Neurol 1988;100:332–40.

Sakuma K, Hashimoto I. High-frequency magnetic oscillations evoked by posterior tibial nerve stimulation. NeuroReport 1999;10:227–30.

Sakuma K, Sekihara K, Hashimoto I. Neural source estimation from a time-frequency component of somatic evoked high-frequency magnetic oscillations to posterior tibial nerve stimulation. Clin Neurophysiol 1999;110:1585–8.

Schnitzler A, Witte OW, Cheyne D, Haid G, Vrba J, Freund HJ. Modulation of somatosensory evoked magnetic fields by sensory and motor interferences. NeuroReport 1995;6:1653–8.

Shimazu H, Kaji R, Tsujimoto T, Kohara N, Ikeda A, Kimura J, Shibasaki H. High-frequency SEP components generated in the somatosensory cortex of the monkey. NeuroReport 2000;11:2821–6.

Sloper JJ, Johnson P, Powell TP. Selective degeneration of interneurons in the motor cortex of infant monkeys following controlled hypoxia: a possible cause of epilepsy. Brain Res 1980;198:204–9.

Swadlow HA. Influence of VPM afferents on putative inhibitory interneurons in S1 of the awake rabbit: evidence from cross-correlation, microstimulation, and latencies to peripheral sensory stimulation. J Neurophysiol 1995;73:1584–99.

Swadlow HA, Beloozerova IN, Sirota MG. Sharp, local synchrony among putative feed-forward inhibitory interneurons of rabbit somatosensory cortex. J Neurophysiol 1998;79:567–82.

Tanosaki M, Kimura T, Takino R, Iguchi Y, Suzuki A, Kurobe Y, Haruta Y, Hoshi Y, Hashimoto I. Movement interference attenuates somatosensory high-frequency oscillations: contribution of local axon collaterals of 3b pyramidal neurons. Clin Neurophysiol 2002;113:993–1000.

Yamada T, Kameyama S, Fuchigami Y, Nakazumi Y, Dickins QS, Kimura J. Changes of short latency somatosensory evoked potential in sleep. Electroencephalogr Clin Neurophysiol 1988;70:126–36.

Parkin-positive autosomal recessive juvenile parkinsonism with α-synuclein-positive inclusions

Shoichi Sasaki, MD; Akiko Shirata, MD; Kiyomi Yamane, MD; and Makoto Iwata, MD

Abstract—*Objective:* To report an autopsy case of an autosomal recessive juvenile parkinsonism patient with a homozygous exon 3 deletion in the *parkin* gene and α-synuclein-positive inclusions. *Methods:* The representative areas of the brain were embedded in paraffin, stained with hematoxylin-eosin, Klüver-Barrera, and Gallyas-Braak stainings. Immunohistochemically, some of the specimens were used for immunostaining with the antibodies to α-synuclein, ubiquitin, and phosphorylated tau (AT8). Immunoreaction was visualized by the streptavidin-biotin-peroxidase complex method. *Results:* Histologically, the lesions of the brain were limited to the dopaminergic neuron system such as the substantia nigra (SN) and locus ceruleus. Melanin-containing neurons in the pars compacta of the SN were moderately to severely depleted, accompanied by gliosis. In the locus ceruleus, neurons were mildly decreased and extraneuronal melanin pigments were seen. Lewy bodies were not observed in the neuropils of the pars compacta of the SN or locus ceruleus. However, basophilic inclusion bodies were only occasionally observed in the neuropils of the pedunculopontine nucleus in the mesencephalic reticular formation. Immunohistochemistry with antibodies to α-synuclein and ubiquitin showed α-synuclein- and ubiquitin-positive inclusions in the neuropils of the pedunculopontine nucleus, which had a doughnut or round shape. *Conclusions:* A variety of *parkin* gene abnormalities may produce pathologic differences in the degree and distribution of neuronal degeneration, including the absence or presence of Lewy bodies. A relationship between *parkin*-induced parkinsonism and idiopathic Parkinson disease (PD) may exist.

NEUROLOGY 2004;63:678–682

Mutations in the *parkin* gene are a major cause of autosomal recessive juvenile parkinsonism (ARJP) and isolated juvenile-onset Parkinson disease (PD).[1,2] ARJP, one of the most common familial forms of PD, is characterized by selective dopaminergic neuronal loss and the absence of Lewy bodies.[3] However, limited data are available on neuropathologic findings in ARJP patients with mutations in the *parkin* gene,[4-8] and histopathologic findings vary. We report an autopsy case of an ARJP patient with a homozygous exon 3 deletion in the *parkin* gene and α-synuclein-positive inclusions, suggesting a close relationship between ARJP and idiopathic PD.

Methods. *Patient 1.* The clinical features and gene analysis of this patient have been reported.[9] She initially noticed gait disturbance at age 33 years. Several years later, resting tremor of both hands and feet developed. At age 41 she was diagnosed with PD, was treated with levodopa and trihexyphenidyl, and improved. At age 55 she came to our hospital because of deterioration of hypokinesia, gait impairment, and development of dyskinesias of the limbs and trunk. Levodopa was markedly efficacious. There were fluctuations of symptoms and amelioration after sleep. She was admitted because of slow progression of festinating and frozen gait, and levodopa-induced choreic dyskinesia of limbs and trunk. At the time of admission she was alert and nondemented and had no psychiatric manifestations. Neurologic examination showed moderate postural tremor and rigidity of limbs, and choreic dyskinesia of limbs and trunk. Dystonic posture with bilateral extension of big toes was observed. The deep tendon reflexes were normal in the upper extremities and abolished in the legs. The plantar responses were bilaterally flexor. Sensation was normal except for numbness in the bilateral calves. There was no autonomic dysfunction. SPECT, brain MRI, and EEG showed no abnormality. There was reduced voltage of sensory nerve action potential (SNAP) in the bilateral sural nerves and delayed N9 in short somatosensory evoked potential on nerve conduction examination, suggesting the presence of peripheral neuropathy. After discharge, she was followed as an outpatient but was readmitted because of acute renal failure due to dehydration and deterioration of hypokinesia. After admission, pneumonia and sepsis developed, followed by disseminated IV coagulation, bacterial shock, and nephrotic syndrome. The patient died of respiratory failure at age 70, with a clinical course of about 37 years. Autopsy was performed 11 hours after death.

Patient 2. The elderly sister of Patient 1 had a similar disease. She first noticed resting tremor in both hands at age 36, followed by gait disturbance. At age 43 she was diagnosed with PD, and she improved after levodopa and trihexyphenidyl treatment. At age 47 propulsion developed with difficulty of walking. At age 57 she was admitted to our hospital because of deterioration of choreic movement of the limbs and trunk. On neurologic examination, she was alert, fully oriented, and not demented, with no psychiatric manifestations. She had monotonous voice and difficulty swallowing. Manual muscle test showed slight weakness in all limbs and was graded 4/5. She showed resting and postural tremor (about 3 Hz), rigidity of limbs, and choreic movement of limbs and trunk. The deep tendon reflexes were normal in the upper extremities and reduced in the lower extremities. The plantar responses were bilaterally flexor. Sensation was normal except for numbness in the bilateral caves. Standing and walking was impossible because of postural instability. No SNAP was obtained

From the Department of Neurology (Drs. Sasaki and Iwata), Neurological Institute, Tokyo Women's Medical University, Tokyo; and Department of Neurology (Drs. Shirata and Yamane), Neurological Institute, Ohta-Atami Hospital, Koriyama, Japan.

This work was supported by a Grant-in-Aid for General Scientific Research (C) from the Japanese Ministry of Education, Science and Culture.

Received February 16, 2004. Accepted in final form April 30, 2004.

Address correspondence to Dr. Shoichi Sasaki, Department of Neurology, Neurologic Institute, Tokyo Women's Medical University, 8-1 Kawada-cho, Shinjuku-ku, Tokyo 162-8666, Japan; e-mail: ssasaki@nij.twmu.ac.jp

at the sural nerve on nerve conduction examination. There was no abnormality on EEG, SPECT, or brain CT. She showed good response to levodopa and dopamine agonist, and choreic movement was improved by tiapride. There were fluctuations of symptoms and amelioration after sleep. She was followed as an outpatient but died suddenly of unknown causes at age 63. Autopsy was not performed.

Pathology. The left side of the brain of Patient 1 was dissected and stored at −70 °C. The right side of the brain was fixed in neutral buffered formalin, and the representative areas were embedded in paraffin, stained with hematoxylin-eosin, Klüver-Barrera, and Gallyas-Braak stainings. Immunohistochemically, some of the specimens were used for immunostaining with the antibodies to α-synuclein (LB509, 1:2000; a gift from Dr. T. Iwatsubo), ubiquitin (polyclonal, rabbit, 1:100; Dako, Glostrup, Denmark), and phosphorylated tau (AT8) (monoclonal, mouse, 1:1000; Innogenetics, Ghent, Belgium). Immunoreaction was visualized by the streptavidin-biotin-peroxidase complex method. The final chromogen was 3, 3'-diaminobenzidine tetrahydrochloride.

Gene analysis. Gene analysis of the *parkin* gene was also performed in Patient 1. Genomic DNA was extracted from peripheral leukocytes. The 12 exons, including the flanking intronic sequences, were amplified by individually using the same primer pairs as described previously.[10] The PCR products were run through a 2% agarose gel in 1xTAE buffer (1xTAE = 0.04 *M* tris-acetate, 0.001 *M* ethylenediaminetetraacetic acid, pH 8.0) to determine the presence of the exonic deletions.

Results. *Pathologic findings.* The general pathologic findings were congestive edema of both lungs, bronchopneumonia with pleural effusion, and aspiration of bloody material of the left lung resulting in asphyxia. The brain weighed 1,040 g. There were no abnormalities in the external appearance of the cerebrum, cerebellum, or brain stem. The substantia nigra (SN) showed marked depigmentation. Histologically, the lesions of the brain were relatively limited to the SN and locus ceruleus. Melanin-containing neurons in the pars compacta of the SN were moderately to severely depleted, particularly in the ventrolateral group and the medial part, accompanied by gliosis (figure 1). Some dopaminergic neurons still existed in the intermediate part of the SN. Most of the remaining nigral neurons contained melanin pigments but were atrophic, and free melanin was observed (figure 2). The pars reticulata of the SN was spared. In the locus ceruleus, neurons were mildly decreased and extraneuronal melanin pigments were seen. Lewy bodies were not observed in the SN or locus ceruleus. Inclusion bodies resembling Lewy bodies but more basophilic were occasionally observed in the neuropils of the pedunculopontine nucleus in the mesencephalic reticular formation (figure 3). No neurofibrillary tangles, neuritic plaques, or abnormal structures stained with Gallyas-Braak staining were demonstrated. There were no abnormalities in the cerebral cortex, basal ganglia, thalamus, cerebellum, or other brain stem nuclei. Immunohistochemically, α-synuclein-positive (figure 4) and ubiquitin-positive (figure 5) inclusions were occasionally found in the neuropils of pedunculopontine nucleus. These inclusion bodies had a doughnut or round shape. No α-synuclein- and ubiquitin-positive inclusions were seen in other regions of the brain such as the SN, locus ceruleus, or subthalamic nucleus. No immunoreactivity of phosphorylated tau was found in any region of the brain.

Genetic findings. A homozygous exon 3 deletion in the *parkin* gene was found in Patient 1.

Discussion. So far, neuropathologic examination has been reported separately in five ARJP patients with mutations in *parkin*.[4-8] An absence of Lewy bodies and a severe generalized loss of pigmented neurons in the SN were common in four of the five ARJP patients.[4-8] However, the discrepancies include the following: one of four brains (the specific location of *parkin* mutation is not described) showed neurofibrillary tangles and argyrophilic astrocytes in the cerebral cortex and brain stem nuclei[4]; the second brain, with a homozygous exon 4 deletion in the *parkin* gene, showed involvement of the SN pars reticulata[5]; the third one (probably with a compound heterozygous combination of two mutations—the amino acid change Lys211Asn in exon 6 and an exon 3 deletion)—showed neuronal loss in parts of the spinocerebellar system together with abnormal tau protein deposition[6]; and the fourth, with a single heterozygous C212Y mutation (heterozygous carrier of C212Y mutation of the *parkin* gene), showed tau aggregates consistent with clinical and pathologic features of progressive supranuclear palsy.[7] Autopsy reports confirmed the absence of Lewy bodies in *parkin*-related disease cases and support the hypothesis that parkinsonism due to *parkin* gene mutations and idiopathic PD result from distinct etiologic causes. By contrast, the remaining brain, with an exon 7 R275W substitution in addition to a novel 40 bp exon 3 deletion, showed Lewy bodies not only in the SN and locus ceruleus but also in the nucleus basalis of Meynert and the amygdalo-hippocampal region, first indicating that compound heterozygous *parkin* mutations may lead to early-onset PD with Lewy body pathology.[8] The brain of the present patient showed a homozygous exon 3 deletion in the *parkin* gene. We confirmed the severe loss of dopaminergic neurons of the SN, the presence of inclusion bodies resembling Lewy bodies, and α-synuclein-positive and ubiquitin-positive inclusions in the neuropils of the pedunculopontine nucleus in the mesencephalic reticular formation. However, the inclusion bodies were somewhat basophilic, and therefore differed from Lewy bodies, which show an eosinophilic tint. The reason for the absence of Lewy bodies in the SN commonly involved in PD is unclear, but may reflect the severe loss of melanin-bearing dopaminergic neurons. Mutation in the gene encoding *parkin* in our patient differs from that of a reported ARJP patient with Lewy bodies,[8] suggesting variability between mutations in terms of *parkin* and neuropathologic findings. Thus, parkin disease is a distinct genetic entity whose clinical and pathologic features overlap somewhat with those of idiopathic PD.[11] The diversity of clinical and histopathologic findings may represent pathologic heterogeneity among parkinsonism associated with *parkin* gene mutations.

Parkin is a protein of unknown function, but sequence homology to ubiquitin in its N terminus suggests that parkin has E3 ubiquitin ligase and may function in the ubiquitin protein degradation pathway.[12] In view of the presence of ubiquitin epitopes in Lewy bodies, the ligase activity of parkin, and the

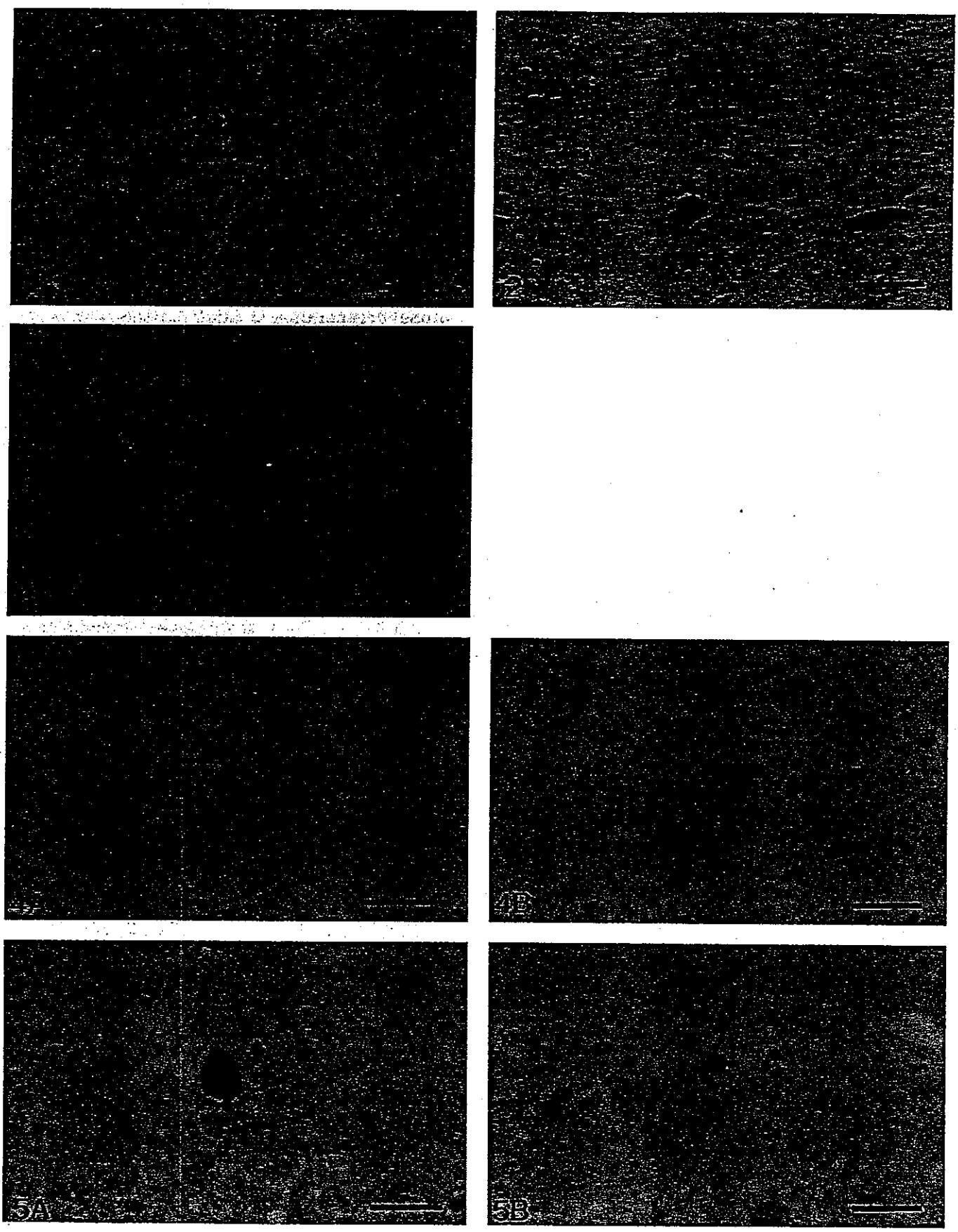

Figure legends appear on page 681.

10. Kitada T, Asakawa S, Hattori N, et al. Mutations in the *parkin* gene cause autosomal recessive juvenile parkinsonism. Nature 1998;392: 605–608.
11. Khan NL, Graham E, Critichley P, et al. Parkin disease: a phenotypic study of a large case series. Brain 2003;126:1279–1292.
12. Shimura H, Hattori N, Kubo S, et al. Familial Parkinson's disease gene product, parkin, is a ubiquitin-protein ligase. Nat Genet 2000;25:302–305.
13. Shimura H, Hattori N, Kubo S-I, et al. Immunohistochemical and subcellular localization of Parkin protein: absence of protein in autosomal recessive juvenile parkinsonism patients. Ann Neurol 1999;45:668–672.
14. Dawson TM. New animal models for Parkinson's disease. Cell 2000;101: 115–118.
15. Shimura H, Schlossmacher MG, Nattori N, et al. Ubiquitination of a new form of α-synuclein by parkin from human brain: implications for Parkinson's disease. Science 2001;293:263–269.
16. Haass C, Kahle PJ. Parkin and its substrates. Science 2001;293:224–225.
17. Chung KKK, Zhang Y, Lim KL, et al. Parkin ubiquitinates the α-synuclein-interacting protein, synphilin-1: implications for Lewy-body formation in Parkinson's disease. Nat Med 2001;7:1144–1150.
18. Saito Y, Kawashima A, Ruberu NN, et al. Accumulation of phosphorylated α-synuclein in aging human brain. J Neuropathol Exp Neuol 2003;62:644–654.
19. Hardy J, Cookson MR, Singleton A. Genes and parkinsonism. Lancet Neurol 2003;2:221–228.
20. Corti O, Brice A. Parkin and Parkinson's: more than homonymy? Ann Neurol 2001;50:283–285.

Acta Neuropathol (2004) 107:452–460
DOI 10.1007/s00401-004-0838-y

REGULAR PAPER

Shoichi Sasaki · Hitoshi Warita · Koji Abe · Makoto Iwata

Slow component of axonal transport is impaired in the proximal axon of transgenic mice with a G93A mutant SOD1 gene

Received: 26 September 2003 / Revised: 14 January 2004 / Accepted: 14 January 2004 / Published online: 17 March 2004

Abstract The purpose of this study was to determine whether slow axonal transport of neurofilaments (NFs) is impaired in the spinal cord of G93A Cu/Zn superoxide dismutase (SOD1) mutant transgenic mice expressing a relatively low mutant protein (gene copy 10) and, if so, how the impairment occurs in this animal model. Transgenic mice were killed at the ages of 24, 28 and 32 weeks, and the cervical and lumbar spinal cords were examined under an electron microscope. Age-matched non-transgenic wild-type mice served as controls. At 24 weeks (early presymptomatic stage), anterior horn cells were well preserved. The earliest morphological changes were mild vacuolar changes in the neuronal processes, particularly in proximal axons. At 28 weeks (late presymptomatic stage), mild neuronal loss of anterior horn neurons was observed. Vacuolar changes were more prominent in the proximal axons, including swollen axons (spheroids) and neuropils of the anterior horns. Vacuoles in the axons were frequently large enough to occupy almost the entire axonal caliber. The anterior roots were degenerative, showing vacuolar changes and myelin ovoids. Lewy body-like inclusions (LIs) consisting of filaments thicker than NFs (about 1.5 times larger in diameter) were frequently demonstrated in the neuronal processes including swollen axons (spheroids) and occasionally in the somata. At 32 weeks (symptomatic stage), the anterior horns showed a moderate to severe neuronal loss accompanied by prominent astrogliosis. Cord-like swollen axons consisting of accumulated NFs and many neurofilamentous accumulations were frequently observed in the anterior horn. Vacuolar changes were less prominent or disappeared in the neuropils of the anterior horns and the anterior roots, whereas LIs were frequently demonstrated within the neuronal processes including the cord-like swollen axons. In the anterior roots, degenerative changes such as marked fiber loss and frequent myelin ovoids were remarkable. No accumulation of NFs or mitochondrial vacuolation was detected in somata or proximal dendrites at any stage. These findings suggest that the slow component of axonal transport in the proximal axons is impaired at an early stage in this transgenic mouse model, and that the impairment is probably caused by a mechanical impediment of NFs, or by the accumulation of NFs in the proximal axon, as a result of the obstruction of the axonal flow that initially occurs by vacuolar changes, and is later exacerbated by accumulation of LIs.

Keywords Amyotrophic lateral sclerosis · SOD1 mutant · Neurofilament · Axonal transport · Vacuolation

S. Sasaki (✉) · M. Iwata
Department of Neurology, Neurological Institute,
Tokyo Women's Medical University,
8-1 Kawada-cho, Shinjuku-ku, 162-8666 Tokyo, Japan
Tel.: +81-3-33538111 ext 39232, Fax: +81-3-52697324,
e-mail: ssasaki@nij.twmu.ac.jp

H. Warita
Department of Neurology, Yonezawa National Hospital,
Yonezawa, Japan

K. Abe
Department of Neurology, Okayama University, Okayama, Japan

Introduction

Accumulations of neurofilaments (NFs) in the cell bodies and proximal axons of motor neurons are a common feature of sporadic amyotrophic lateral sclerosis (ALS) [8], familial ALS [9, 15], and transgenic (Tg) mice expressing the Cu/Zn superoxide dismutase (SOD1) mutation [10]. The aberrant accumulation of NF proteins, which has been implicated in the development of motor neuron disease (MND), may be an indication of abnormal transport of these large proteins [10]. Moreover, transgenes encoding mutant NF subunits could directly cause selective degeneration and death of motor neurons and the ensuing axonal disorganization [12]. Previous findings suggest that damage to NFs might be directly involved in ALS pathogenesis. However, how these accumulations of NFs are formed and how they contribute to the disease remain unknown. Using electron microscopy, we carried out a

prospective longitudinal pathological study on the spinal cords of Tg mice of a relatively low Tg copy number with a G93A mutant SOD1 gene that were generated in our own laboratories, covering the presymptomatic to symptomatic stages, to determine whether the slow component of axonal transport is impaired in the proximal axons, and, if so, how the impairment occurs.

Materials and methods

Experimental animals and clinical assessment

Tg mice expressing the G93A mutant human SOD1 [7] were originally obtained from the Jackson Laboratory [B6SJL-TgN (SOD1-G93A) 1 Gur[dl], Bar Harbor, Me., USA] and backcrossed to a C57BL/6 background strain by mating hemizygote males with inbred C57BL/6 female mice (C57BL/6CrSlc, Nihon SLC, Shizuoka, Japan) to produce Tg and non-Tg littermates. Backcrossing them onto the black 6 background entirely eliminated the SJL (dysferlin gene-associated FSH dystrophy) background from the colony used for these studies. The Tg progeny was identified by polymerase chain reaction (PCR) amplification of tail DNA with specific primers for exon 4 [14]. These G93A SOD1 mutant mice expressed a relatively low mutant protein (gene copy 10).

At around 32 weeks of age, the G93A Tg mice developed progressive muscle weakness and spasticity in one or more limbs, beginning with a posterior limb. After 1–2 weeks, they could not feed themselves due to severe paralysis expressed by the hyperextension of their hind limbs. The G93A Tg and non-Tg mice were examined simultaneously. Throughout the present study, the mice were treated in accordance with the Helsinki declaration and the guiding principles in the care and use of animals.

Histopathological analysis

Tg mice were divided into three groups: early presymptomatic Tg (aged 24 weeks, n=2), late presymptomatic Tg (aged 28 weeks, n=2), and symptomatic Tg (aged 32 weeks, n=2). Age-matched non-Tg mice served as controls in each group (n=7). All mice were deeply anesthetized with ether and perfused intracardially with heparinized saline (pH 7.4), followed by perfusion with ice-cold 4% paraformaldehyde (Katayama Chemical, Osaka, Japan) in 0.1 M phosphate buffer (pH 7.4). The spinal cords were removed rapidly and post-fixed by immersion in the same fixative (5 days, 4°C). Cross-sections of the spinal cord were embedded in paraffin, sectioned (4 μm), and stained with hematoxylin and eosin (HE), and with cresyl violet.

Immunohistochemistry

Sections (6 μm thick) of the paraffin-embedded spinal cords were deparaffinized, quenched with 3% H_2O_2, treated with nonimmune serum as the blocking reagent, and incubated overnight at 4°C with a mouse monoclonal antibody to rat phosphorylated neurofilament (SMI-31, Sternberger Monoclonals, 1:1,000). Antibody binding was visualized by the biotin-streptavidin peroxidase complex method. The final chromogen was 3,3′-diaminobenzidine tetrahydrochloride.

Ultrastructural study

Six Tg and six non-Tg wild-type mice were killed at the ages of 24, 28, and 32 weeks (n=2 for each group, respectively). All mice were deeply anesthetized with ether and perfused intracardially with heparinized saline (pH 7.4) followed by perfusion with ice-cold 4% paraformaldehyde (Katayama Chemical, Osaka, Japan) and 0.2% glutaraldehyde in 0.1 M phosphate buffer (pH 7.4). The spinal cords were rapidly removed and post-fixed by immersion in the same fixative (5 days, 4°C). Tissues were incubated in 2% osmium tetroxide in 0.1 M cacodylate for 2 h, washed, dehydrated, and embedded in epoxy resin (Epon). Serial semithin sections (1 μm) of the whole transversed spinal cords stained with toluidine blue were examined by light microscopy. Appropriate portions were cut into ultrathin sections and subsequently stained with lead citrate and uranyl acetate for electron microscopic study.

Results

Light microscopic findings

Tg mice

At the age of 24 weeks (early presymptomatic stage), HE and Klüver-Barrera stainings revealed no pathological change. However, in Epon-embedded plastic sections stained with toluidine blue, small vacuolar changes were observed in the neuropils of the ventral portion of the anterior horn, in the axons of the anterior horn, around the central canal, and in the axons of the anterior root exit zone of the anterior column in one of the two mice examined. White matter showed no abnormality in either of these mice.

At the age of 28 weeks (late presymptomatic stage), slight neuronal loss of anterior horn cells was observed at the cervical and lumbar levels. Prominent vacuolar changes were recognized in the same regions showing changes in the early presymptomatic stage. Proximal swollen axons with prominent vacuolar changes shaped like a sausage or a string of beads were frequently found in a longitudinal section (Fig. 1). The anterior roots were degenerative showing vacuolar changes and myelin ovoids, whereas the posterior roots showed no abnormality. Lewy body-like inclusions (LIs) were frequently seen in the neuronal processes including cord-like swollen axons (Fig. 2). Some remaining anterior horn neurons also contained LIs, although they were only occasionally found in the posterior horn (Rexed's lamina V).

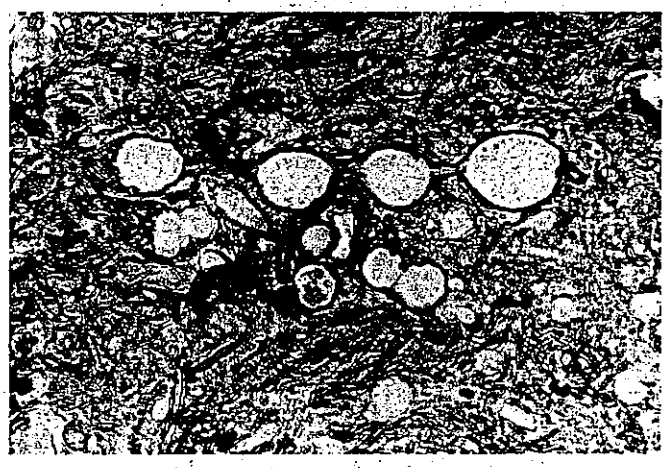

Fig. 1 Proximal swollen axons with prominent vacuolar changes assuming the shape of a sausage or a string of beads in a longitudinal section (late presymptomatic stage). Plastic section, toluidine blue staining. Original magnification ×714

Fig. 2 A Lewy body-like inclusion with a central core is observed in the neuronal process in the neuropils of the anterior horn (late presymptomatic stage). Plastic section, toluidine blue staining. Original magnification ×714

Fig. 3 Proximal swollen axon with prominent vacuolar change shaped like a string of beads is immunostained for phosphorylated NF (SMI-31) (*NF* neurofilament). Original magnification ×714

At the age of 32 weeks (symptomatic stage), the anterior horns showed moderate to severe neuronal loss of anterior horn cells at all levels of the spinal cord. Most remaining anterior horn neurons showed types of degeneration such as central chromatolysis. Vacuolar changes were less prominent or had disappeared, although some persisted in the anterior root exit zone of the anterior column. On the other hand, LIs were frequently observed within the neuronal processes in the anterior horns, including the cord-like swollen axons. Proximal axonal swellings (spheroids) were occasionally found in the neuropils of anterior horns. Myelin ovoid formation was prominent in the white matter of the anterior and lateral columns, especially at the outer zones, and in that of the posterior column adjacent to posterior horns. Anterior roots showed marked degenerative changes such as marked fiber loss and myelin ovoids. Myelin ovoids were also found in the posterior roots, though to a lesser extent.

Immunohistochemically, spheroids or proximal swollen axons with prominent vacuolar changes were positively immunostained for phosphorylated neurofilament (SMI-31) (Fig. 3).

Non-Tg littermates

No vacuolar changes, LIs or swollen axons immunostained for phosphorylated NF were detected in the spinal cord at any age.

Ultrastructural findings

Tg mice

At 24 weeks (early presymptomatic stage), mitochondrial swelling and vacuolation of the inner compartment were observed predominantly in the proximal axons in the anterior root exit zone and anterior root, and in the neuropils of the ventral portion of the anterior horn. Most of these vacuoles were relatively small. In contrast, almost all of the mitochondria in the small myelinated axons in these regions had a normal appearance. Small filamentous aggregates were only occasionally observed in the neuronal processes including the axons in the anterior horns.

At 28 weeks (late presymptomatic stage), mitochondria were frequently swollen and vacuolated in the large myelinated axons of the same regions showing changes in the early presymptomatic stage. Vacuolar changes of various stages, from small focal vacuolar formation in the inner compartment to large vacuoles, were observed in these axons. The vacuoles tended to be larger than those of the early presymptomatic stage. The intermembrane space between the inner and outer membranes was also vacuolated, frequently with large vacuoles. In mitochondria with advanced vacuolation, the vacuolar space was filled with a granular or amorphous substance. Usually, giant vacuoles were accompanied by axonal swellings, and occupied almost the entire axonal caliber, thus blocking the axonal transport with accumulation of mitochondria and misdirected NFs (Fig. 4): accumulated NFs were seen in close proximity to vacuoles or in the axon between the large vacuoles in the longitudinal section of axons. Spheroids consisting of interwoven NFs were frequently observed in the anterior horn and the anterior column (Fig. 5). Filamentous aggregates were frequent, predominantly in the neuronal processes of the anterior horns including the proximal axons (Fig. 6), and, to a lesser extent, in the somata and the dendrites of the anterior horn neurons. The aggregates consisted basically of interwoven intermediate filaments thicker than NF (about 1.5 times larger in diameter). They were composed of filaments that were loosely or compactly packed in the advanced phase, and frequently contained electron-dense granular or amorphous cores in the center. Cord-like swollen axons with or without a myelin sheath consisted of accumulated NFs running parallel to the longitudinal axis, and frequently showed a

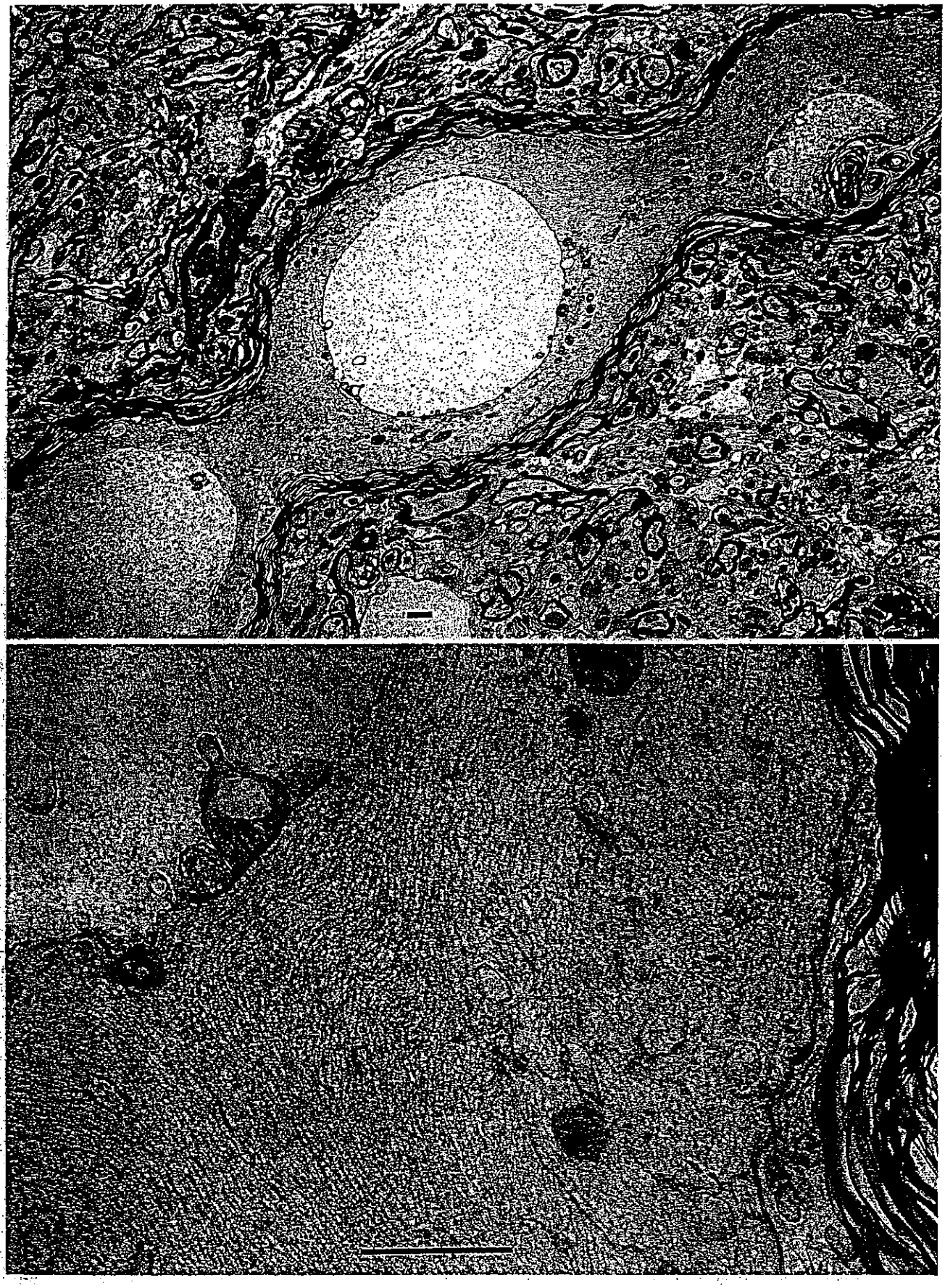

Fig. 4 A Giant vacuoles accompanied by axonal swelling occupy almost the entire axonal caliber. Accumulation of mitochondria attached to the inner membrane of the vacuole is seen (late presymptomatic stage). B Higher magnification of A. Accumulation of misdirected NFs is exhibited in close proximity to vacuoles or between large vacuoles. *Bar* 1 μm

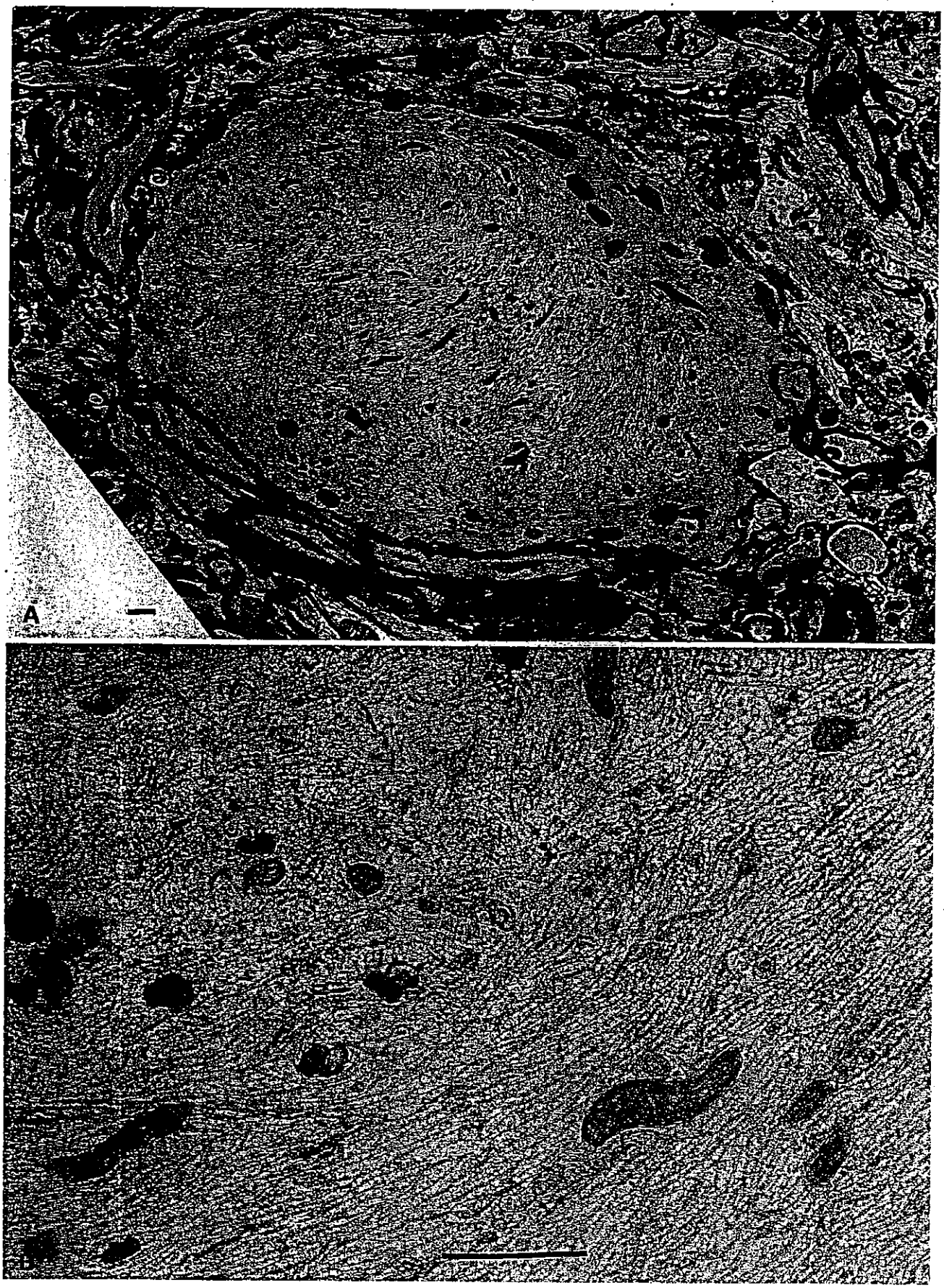

Fig. 5 A A spheroid is observed in the anterior column (late presymptomatic stage). B Higher magnification of A. The spheroid is composed mainly of interwoven NFs with non-vacuolated round or sausage-shaped mitochondria. *Bar* 1 μm